BBA - Bioenergetics 1860 (2019) 155–166

Contents lists available at ScienceDirect

BBA - Bioenergetics

journal homepage: www.elsevier.com/locate/bbabio

Role of the PB-loop in ApcE and phycobilisome core function in cyanobacterium *Synechocystis* sp. PCC 6803☆

Dmitry V. Zlenko[a], Irina V. Elanskaya[a], Evgeny P. Lukashev[a], Yulia V. Bolychevtseva[b], Natalia E. Suzina[c], Elena S. Pojidaeva[d], Irena A. Kononova[a], Aleksey V. Loktyushkin[a], Igor N. Stadnichuk[d,*]

[a] *Faculty of Biology of M.V. Lomonosov Moscow State University, Moscow, Russia*
[b] *A.N. Bach Institute of Biochemistry, Research Center of Biotechnology, Russian Academy of Sciences, Moscow, Russia*
[c] *G.K. Skryabin Insitute of Biochemistry and Physiology of Microorganisms, Russian Academy of Sciences, Puschino, Moscow Region, Russia*
[d] *K.A. Timiryazev Institute of Plant Physiology, Russian Academy of Sciences, Moscow, Russia*

ARTICLE INFO

Keywords:
Phycobilisome
Cyanobacteria
ApcE protein
PB-loop

ABSTRACT

The phycobilisome (PBS) is a giant highly-structured pigment-protein antenna of cyanobacteria and red algae. PBS is composed of the phycobiliproteins and several linker polypeptides. The large core-membrane linker protein (L_{CM} or ApcE) influences many features and functions of PBS and consists of several domains including the chromophorylated PB-domain. Being homologous to the phycobiliprotein α-subunits this domain includes a so-called PB-loop insertion whose functions are still unknown. We have created the photoautotrophic mutant strain of the cyanobacterium *Synechocystis* sp. PCC 6803 with lacking PB-loop. Using various spectral techniques we have demonstrated that this mutation does not destroy the PBS integrity and the internal PBS excitation energy transfer pathways. At the same time, the deletion of the PB-loop leads to the decrease of connectivity between the PBS and thylakoid membrane and to the compensatory increase of the relative photosystem II content. Mutation provokes the violation of the thylakoid membranes arrangement, the inability to perform state transitions, and diminishing of the OCP-dependent non-photochemical PBS quenching. In essence, even such a minute mutation of the PBS polypeptide component, like the PB-loop deletion, becomes important for the concerted function of the photosynthetic apparatus.

1. Introduction

The phycobilisomes (PBSs) are giant (5–20 MDa) phycobiliprotein antenna complexes associated with the thylakoid membranes of cyanobacteria and red algae. The phycobiliproteins are formed by α and β polypeptides with covalently bound phycobilin chromophores and self associated in ($\alpha\beta$) monomers, than in discoidal $(\alpha\beta)_3$ trimers, and finally in $(\alpha\beta)_6$ hexamers. PBS consists of two main structural subcomplexes: the central core composed of trimeric allophycocyanin (APC) discs stacked into cylinders, and the lateral cylindrical rods radiating from the core. The rods consist of hexameric phycocyanin (PC) and/or some other phycobiliproteins. Several colorless and chromophorylated linker polypeptides are associated with the phycobiliprotein discs optimizing energy transfer and maintaining PBS integrity (for comprehensive reviews see Refs. [1-5]).

The hemidiscoidal PBS of the model cyanobacterium *Synechocystis* sp. PCC 6803 (hereafter *Synechocystis*), has the tricylindrical core and six lateral rods. Each core cylinder is composed of four APC trimers. Two tightly packed parallel basal cylinders of the core contact the thylakoid membrane, whereas one upper cylinder is located in the central furrow between them. The external APC discs bind small colorless ApcC linker polypeptide [6,7]. The bottom core cylinders contain minor APCs: the *apcD* gene product or the α-subunit of APC B [8,9], the *apcE* gene product or core-membrane linker protein, L_{CM} [10], and the *apcF* gene product or β^{18} polypeptide [9,11]. Similar to the bulk APCs all the minor polypeptides carry one but red-shifted phycocyanobilin chromophore.

For today, the precise study of the PBS architecture by the single-particle electron microscopy [12-14] and various other methods [1-6,15] is limited by insufficient data on ApcE protein spatial structure [13]. The ApcE is known to be the largest and most complicated polypeptide of the PBS [2,10]. Its molecular mass varies in the range of

☆ The work was in part supported by RFBR grant for young scientists number 18-34-00082.
* Corresponding author.
E-mail address: stadnichuk@mail.ru (I.N. Stadnichuk).

https://doi.org/10.1016/j.bbabio.2018.10.004
Received 25 June 2018; Received in revised form 4 October 2018; Accepted 29 October 2018
Available online 07 November 2018
0005-2728/

70–128 kDa depending on the organism [1]. Biochemical studies of the isolated ApcE are rare due to its poor solubility and easy precipitation [16-19]. The *apcE* gene, encoding the L_{CM}, has been cloned and sequenced [10,20,21]. The C-terminal part of *Synechocystis* ApcE contains three structural REP domains of ~ 120 residues long and unstructured Arms between them [1,10,20,22]. The N-terminal domain of ApcE (PB-domain) is 47–55 % similar to the αAPC subunit; their secondary and tertiary structures are also similar according to the X-ray and homology modeling results [23-25]. The chromophorylated PB-domain replaces one αAPC in one of the middle APC trimers in each of the core basal cylinders [9,26,27] and includes an unstructured loop (PB-loop) of approximately 50–70 amino acid residues long. The PB-loop has no homology to other parts of PBS [10] and most probably sticks out of the PBS core surface [22,24,25,28]. The complex molecular structure of ApcE hinders its structural analysis. The whole ApcE was not yet crystallized, but some crystallographic data were obtained for the isolated PB-domain lacking the hydrophobic PB-loop [24] and for some of the isolated REP domains (PDBIDs: 2KY4, 2L06, 3OSJ, and 2OHW).

Since ApcE can be copurified with the isolated chlorophyll-containing membrane fractions [29,30], it was postulated that the ApcE protein anchors PBS to the thylakoid membrane (hence the another name “anchor” polypeptide, or “core-membrane linker” [1,28]). In *Synechocystis*, the number of the REP domains equals the number of the APC cylinders in the core [1,10,20,22] and the structure of the REP domains is highly similar to one of the two domains of the rod PBS linkers [4]. It was proposed that ApcE fastens together the APC discs in the core cylinders. Due to the strong overlap of the PBS fluorescence emission with the chlorophyll absorption, ApcE together with ApcD are generally accepted to be the excitation energy transmitters from the bulk PBS chromophores to the photosynthetic reaction centers of photosystems II and I (PSII and PSI; reviewed in Refs. [1,30,31]).

In cyanobacteria, the mechanism of non-photochemical quenching differs from that in the green plants [32]. The carotenoid molecule is incorporated into the water-soluble orange carotenoid protein (OCP) rather than to the membrane antenna complex [33]. The PB-domain of ApcE is an obvious candidate for the role of OCP binding site, as the direct interaction of OCP and ApcE was demonstrated *in vitro* [19], and in the cross-linking experiments [34,35], although some other possibilities are still under discussion [33-36].

Functional role of ApcE was investigated by gene disruption: several *apcE* lacking cyanobacterial strains were obtained but it turned out that in this case the PBSs did not assemble [37-40]. There were several attempts to delete the ApcE chromophore by site-directed mutagenesis: the phycocyanobilin-binding Cys190 residue has been replaced by serine [41-44]. However, in these mutants the chromophore became noncovalently self-associated with the corresponding pigment pocket of ApcE. Its fluorescence emission peak was red-shifted from 680 to 710–715 nm, as in the ApcE2 protein from the FARLiP cyanobacterial species (reviewed in Ref. [45]). In another kind of the ApcE mutant with deleted whole PB-domain, the assembled hemidiscoidal PBSs were not able to associate with the thylakoid membrane and therefore the cells have lost the PBS-dependent functions [46]. At the same time, the steady-state fluorescence and absorption spectroscopy at the room temperature did not reveal any effects on PBS assembly or energy transfer functions in the PB-loop lacking strain of the cyanobacterium *Synechocystis* sp. PCC 6714 [40].

Therefore, in order to evaluate the role of the PB-loop in functioning of the PBSs and whole pigment apparatus of cyanobacteria, we have created the mutant of *Synechocystis* (ΔPB-loop mutant) with an in frame deletion of the PB-loop. The objective of this study was in an in-depth analysis of the ΔPB-loop mutant with respect to the photosynthetic apparatus function.

2. Materials and methods

2.1. Cultivation conditions

The cyanobacterium *Synechocystis* sp. PCC 6803 wild type (WT) and its ΔPB-loop mutant were grown autotrophically for 4–5 days at 30 °C with constant stirring in standard liquid BG-11 medium with the doubled concentration of sodium nitrate under continuous Phillips cool-white fluorescent light of 40 μmol $m^{-2} s^{-1}$. The ΔPB-loop mutant was maintained in the presence of 20 μg mL^{-1} of chloramphenicol and 100 μg mL^{-1} of kanamycin. Cultures in the late exponential phase (Fig. S1A) were harvested and used for further experiments.

2.2. Construction of the ΔPB-loop mutant

To generate the ΔPB-loop construct without frameshift, we deleted 253–429 bp DNA fragment from the *apcE* start codone. The first DNA fragment with artificial restriction sites for *Kpn*I and *Eco*RI containing 1012 bp upstream of the *apcE* gene and 252 bp from the start of the *apcE* gene was amplified with the primers 5′ -TTGGTACTCTGGTGTGTTGT AGCC-3′ and 5′ -TAGAATTCGTAGGAGAGGGGGGAAC-3′. The second fragment carrying the restriction sites for *Eco*RI and *Bam*HI, containing 431–871 bp fragment of *apcE* was amplified with the primers 5′ -TTG AATTCTACGGTCCCAGCAACAT-3′ and 5′ -TAGG-ATCCAAAGGTGGTG ATGAACT-3′. Both fragments were cross-linked at the *Eco*RI site and inserted into the pBluescript II SK(+) plasmid at the *Kpn*I/*Bam*HI sites. The kanamycin resistance cassette was inserted upstream from the *apcE* gene at the *Sal*I site. Then, the terminal part (starting from the *Bgl*II site) of the inserted *apcE* gene fragment was replaced by the *Bgl*II/*Xba*I fragment containing the rest part of the full-length *apcE* gene and the downstream insertion of the chloramphenicol resistance cassette, as described earlier [46]. The WT cells of *Synechocystis* were transformed with recombinant plasmid carrying the *apcE* gene with PB-loop deletion to yield Km^R/Cm^R clones. The Km^R/Cm^R transformants were subcultured in presence of the increasing concentrations of the antibiotics to segregate the mutant genome copies. Segregation was confirmed by PCR with primers specific for the flanking regions of deletion: Fw: CCGTCGCAGAGCACACCATC and Rev: TGCTTGCGGTAGAGGGGA (Figs. 1, S1B) and by the sequencing (Fig. S2). Three independently segregated mutant strains were used for the analysis.

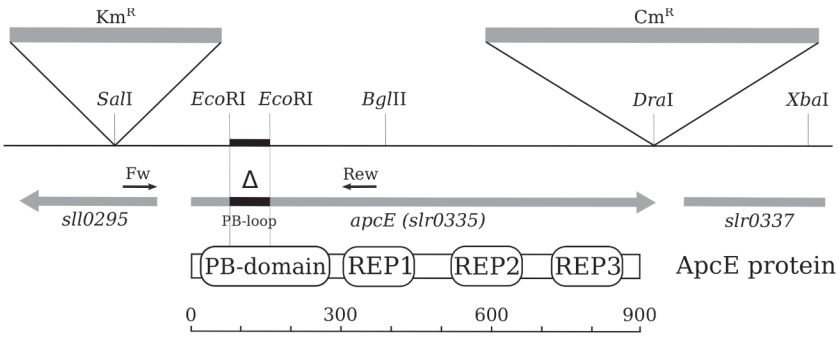

Fig. 1. The *apcE* locus in the *Synechocystis* sp. PCC 6803 genome (top) and the domain structure of the ApcE protein (bottom). The region deleted in the mutant strain is marked as Δ. Km^R corresponds to the kanamycin resistance cassette, Cm^R denotes chloramphenicol resistance cassette. Fw and Rew arrows indicate the position of the PCR primers used for the segregation quality confirmation.

2.3. Phycobilisomes isolation

The PBSs were isolated according to the method of Glazer [47]. The WT and mutant *Synechocystis* cells were harvested by centrifugation (10 min, 7 000 rpm), than washed twice in 0.75 M K-phosphate buffer, pH 7.6 and collected by centrifugation (15 min, 10 000 rpm). Then cells were resuspended in the same buffer and passed twice through the French press Thermo Cell Disrupter at 20 000 psi. Triton X-100 was added to the suspension to a final concentration of 2 % (v/v) to release the PBSs from the thylakoid membranes. After 60 min incubation (20 °C) at constant shaking, the unbroken cells and debris were removed by centrifugation (30 min, 15 000 rpm). The supernatant was loaded onto a linear (0.25–1.0 M) sucrose density gradient in 0.75 M K-phosphate buffer (pH 7.6) for ultracentrifugation at 140 000 *g* for 3 h (37 000 rpm, Beckman 70 Ti rotor, 16 °C). A linear sucrose gradient was prepared from 13 ml of 0.25 M and 13 ml of 1.0 M sucrose solutions in 0.75 M K-phosphate buffer using a gradient mixer (Biocompare, USA). After the ultracentrifugation, the material was collected from the bottom of each tube using a thin needle and roller pump. The gathered narrow blue-colored zone was used for further analysis. The sucrose concentration was measured using PZO RR 11 manual refractometer (Poland).

2.4. Protein electrophoresis

The PBS-containing fractions were diluted by 0.75 M K-phosphate buffer to reduce the sucrose concentration in the sample to 0.2 M. The proteins were then precipitated by the solid ammonium sulfate to a final concentration of 30 %. After collection by centrifugation (30 min, 16, 000 rpm), the precipitate was resuspended in 50 μ L of distilled water and dialyzed overnight to remove the rest of ammonia. Aliquots of the PBS solution were mixed with equal volume of the sample buffer (62.5 mM Tris–HCl, pH 6.8, 2 % SDS, 10 % glycerol, 5 % β-mercaptoethanol, 0.004 % bromphenol blue), and then heated to 70 °C for 5 min. Proteins were analyzed by 10 % Tricine-SDS-PAGE [48] in BioRad Mini Protean System (0.75 × 75 mm). The gels were stained in colloidal Coomassie brilliant blue G.

2.5. Absorption spectra measurements

The room temperature absorption spectra of the cells and isolated PBSs were recorded using a modified Hitachi-557 double beam spectrophotometer (Japan) with the slit width of 4 nm in 5 mm cuvettes or a Varian 2300 UV–Vis spectrophotometer (USA) with a slit width of 2 nm in 2 mm cuvettes for the samples with high scattering property. The 77 K absorption spectra of the isolated PBSs were measured using standard Hitachi-557 spectrophotometer sample holder with a slit set to 2 nm. To minimize the light scattering of the frozen samples they were diluted with glycerol to the final concentration of 60 %. Chlorophyll concentration was determined according to Lichtenthaler [49].

2.6. Steady-state fluorescence spectra measurements

The fluorescence emission spectra were recorded with a Fluorolog-3 instrument (Horiba Jobin Ivon, Japan). Cell spectra were measured in the growth culture medium and the isolated PBS spectra — in 0.75 M K-phosphate buffer (pH 7.6) at 0.69 M sucrose concentration immediately after gradient ultracentrifugation to avoid dissociation of the PBSs. The room temperature measurements were performed in standard cuvettes with 5 mm optical path, while the 77 K measurements — in glass tubes with an internal diameter of 2 mm. The spectra were recorded upon excitation at 440 nm (chlorophyll) or 580 nm (PBS). The bandwidth was 3 nm for the excitation light and 2 nm for the collected light. The individual traces were averaged, baseline-corrected and smoothed by the instrumental software. Optical density of the cell and isolated PBS samples was equal to 0.1 at 678 and 620 nm, respectively.

For the measurements of the OCP-dependent non-photochemical PBS fluorescence quenching, the samples of the WT *Synechocystis* and ΔPB-loop mutant cells were either adapted to the darkness for 20 min or were illuminated with intense (1100 μmol $m^{-2} s^{-1}$) blue-green light for 10 min to induce the $OCP^O \rightarrow OCP^R$ phototransformation. White light from the 650 W halogen lamp (OSRAM) was filtered through the 430–540 nm bandpass and IR-cutoff KG SCHOTT glass filters to obtain the blue-green light.

The state transitions in the WT *Synechocystis* and mutant cells were monitored in the steady-state spectra by the low temperature fluorescence emission measurements under the PBS excitation. The samples were dark-adapted for 15 min to induce the state 2. The state 1 was induced by a subsequent 3 min exposure to the far-red light of ~ 100 μmol $m^{-2} s^{-1}$ generated by the KS-18 cut-off glass filter (LOMO, Russia) and 650 W halogen lamp (OSRAM). The cells were frozen in liquid nitrogen in presence of 20 μM DCMU after adapting to the dark or to the corresponding illumination and used for measurements [50].

2.7. PAM fluorescence measurements

The kinetics of the PSII fluorescence induction in the WT *Synechocystis* and mutant cells were monitored using PAM-101 fluorometer (Walz, Germany). The modulated 1.6 kHz low intensity measuring light of 1 μmol $m^{-2} s^{-1}$ had a maximum at 650 nm and the fluorescence was detected at wavelengths beyond 700 nm. The fluorescence induction kinetics were measured following the switch on of the 580 nm actinic light of 80 μmol $m^{-2} s^{-1}$ provided by a KL-1500 illuminator (Schott, Germany) with the appropriate interference bandpath filter (BPF-580, half-width 35 nm, Photooptic, Russia). The time of the cell samples dark adaptation was 15 min, illumination time was 50 s. Measurements were carried out at a chlorophyll concentration of 10 μg/mL in 1 cm stirred cuvette in presence of 20 μM DCMU. The intensity of the actinic light was controlled by the Quantitherm quantometer (QRT1, Hansatech, Germany).

2.8. Photooxidation of P700

The redox transitions of P700 were evaluated according to the changes of the absorbance at 810 and 870 nm measured at room temperature with a modulated detection system consisting of a PAM-101 control unit and a dual-wavelength emitter-detector unit ED-P700 DW (Walz, Germany) [51]. The high power LEDs (620 and 730 nm, Walz) were used for the samples excitation. The excitation light intensity was in the range from 15 to 1850 μmol $m^{-2} s^{-1}$ that was controlled using the Optical Power Meter System (Thorlabs, Germany). Measurements of P700 phototransformations were performed in the presence of 20 μ M DCMU added to the samples after 15 min of the dark adaptation. A chlorophyll concentration was 10 μ g/mL. The P700 photooxidation and $P700^+$ reduction rate constants were calculated as described in the Appendix.

2.9. Steady state oxygen evolution measurements

The PSII-mediated activity of the whole linear electron transport chain was evaluated according to the measurements of the light-dependent oxygen evolution by the cell suspension in culture medium (chlorophyll concentration was 20 μ g per mL) by a Clark-type oxygen electrode (Oxygraph, Hansatech Instruments) in a 1 ml stirred cuvette maintained at 28 °C. The high power LEDs (3 W) were used for the illumination (440 and 590 nm; 160 and 140 μmol $m^{-2} s^{-1}$, correspondingly). Photosynthetic activity was determined as a difference between the net oxygen evolution in the light and oxygen consumption in the following dark.

2.10. Transmission electron microscopy

The cells were collected by centrifugation (10 000 *g*, 15 min) and fixed in a 2 % glutaraldehyde solution in a 0.05 M cacodylate buffer (pH 7.2) for 1 h at 4 °C. Then, the material was washed three times in a 0.05 M cacodylate buffer (pH 7.2) and additionally fixed in a 2 % solution of OsO_4 in the same buffer for 4 h at the room temperature. The dehydrated material was embedded in Epon 812 epoxy resin. Sections were obtained using the Reichert-Jung Ultracut ultramicrotome (Austria). After cutting, the sections were mounted on the support grids, contrasted for 30 min in a 3 % solution of uranyl acetate in 70 % alcohol, additionally contrasted by a lead citrate [52], and examined in the JEM-1200EX transmission electron microscope (JEOL, Japan) at accelerating voltage of 80 kV.

2.11. Statistics

All steady state fluorescence emission and absorption spectra at the room temperature and 77 K were measured in triplicate for the independent samples of cell culture and isolated PBSs. The OCP-induced PBS quenching, fluorescence induction and the P700 photooxidation measurements using PAM-equipment were done 3–5 times. When necessary, the compared WT *Synechocystis* and the mutant samples were thoroughly equalized for PBS and chlorophyll content. Oxygen photoevolution measurements were repeated three times for the independent cell culture samples.

The distances between the adjacent thylakoids in the EM images were measured 30–40 times in each of 40–50 thin sections for WT and the ΔPB-loop cells. The data processing was made using python engine (numpy, scipy), while the plotting was made using matplotlib. The standard deviation was used as a measure of the values dispersion.

3. Results and discussion

3.1. Properties of the ΔPB-loop ApcE polypeptide

The full length of the *apcE* gene in WT *Synechocystis* comprises 896 amino acid residues including the chromophorylated PB-domain of 254 residues [46]. The deleted fragment corresponding to the PB-loop includes 59 residues (Figs. 1, S2). Therefore, the mutant ApcE polypeptide has lost ~ 23 % of the PB-domain length. The multidomain structure of ApcE allowed us to introduce this modification accompanied by only a partial loss of the ApcE functionality. The structural parts of ApcE embracing three Arms and three REP domains were kept intact and were still capable of building up the PBS core. The chromophore-binding residue (Cys190) is localized inside the PB-domain nearby the PB-loop [24], thus its deletion did not affect this residue as well as the phycobilin chromophore directly.

3.2. Mutant strain pigmentation

The ΔPB-loop mutant was phenotypically similar to the WT *Synechocystis* strain and retained its blue-green color slightly inclining to the yellowish one (Fig. S1A). Both growth rate and biomass accumulation were similar for the WT *Synechocystis* and mutant cultures (data not shown).

At the room temperature, the absorption spectrum of the WT *Synechocystis* cells had PBS peak at 625 nm and the chlorophyll peak at 678 nm that is typical of those cyanobacteria the PBS of which are made up of two bulk phycobiliproteins (PC and APC) solely. These two peaks in the absorption spectrum of the ΔPB-loop cells were found to be in an equal proportion with the WT spectrum (Fig. 2). This notable peculiarity distinguishes this mutant from the other phycobiliprotein-deficient strains, which can not completely compensate for the mutation effects and demonstrate a decrease of the PBS peak in the absorption spectra [39]. At the same time, the mutant strain has a higher amount

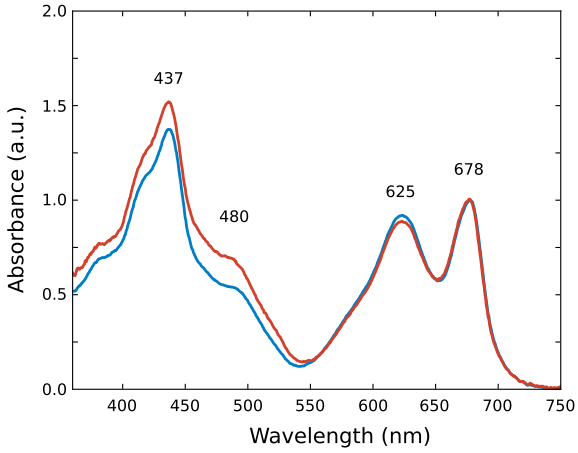

Fig. 2. Room temperature absorption spectra of the WT *Synechocystis* (blue) and ΔPB-loop mutant cells (red). Spectra were normalized at the chlorophyll peak position (678 nm).

of carotenoids (the absorption shoulder at ~ 480 nm) that accounts for the difference in color between the cultures (Fig. S1A). The analogous or greater color changes were observed for various mutants with altered PBS and phycobiliprotein composition brought about by the increased carotenoids content [39,46,53,54].

3.3. PBS assembly

In order to determine how the deletion of the PB-loop influences the phycobiliprotein assembly, the PBSs were isolated from the WT *Synechocystis* and from the ΔPB-loop strain cells. The tubes containing PBSs in sucrose density gradient are shown in Fig. 3, left. In both cases, the sole intensive PBS-containing blue band was located in the gradient at the same sucrose concentration of 0.69 ± 0.02 M. This indicates the presence of the whole PBSs in the mutant cells, as it was observed earlier for ΔPB-loop mutant of *Synechocystis* sp. PCC 6714 [40]. In both tubes, lower sucrose density gradient zones were almost colorless (Fig. 3, left). Therefore, the mutant cells as well as the WT are devoid of free phycobiliproteins.

As the ApcE polypeptide from the ΔPB-loop strain includes the deletion, its electrophoretic mobility has to be greater than in the WT *Synechocystis* sp. PCC 6803. In order to identify and compare the proteins present in the sucrose gradient pigmented zones, the aliquotes of the colored material from the WT and ΔPB-loop samples were analyzed by SDS PAGE (Fig. 3, right). The polypeptides from WT PBS were identified by the analogy with the WT *Synechocystis* protein analysis data [40,46]: ApcE (100 kDa), FNR (48 kDa), rod linkers, CpcC1 and CpcC2 (35 and 33 kDa), CpcG1 rod-core linker (27 kDa), β and α subunits of PC (19.8 and 17.6 kDa, correspondingly), the ApcB subunit (16.2 kDa), the small rod-distal (CpcD, 9.3 kDa), and core-distal (ApcC, 7.7 kDa) linker polypeptides.

The same electrophoretic bands were identified in the ΔPB-loop sample. Thus, the mutant PBS contains both the set of the PC and APC subunits and all the linker polypeptides necessary for the PBS assembly. However, the ApcE polypeptide in this case has a slightly increased electrophoretic mobility, in agreement with ~6 kDa difference between the wild-type and truncated ApcE (Fig. 3, right). This result confirms the accuracy of the genetic manipulations and has been reported earlier for the analogous mutant of *Synechocystis* sp. PCC 6714 [40].

3.4. Spectral properties of the isolated PBSs

The absorption spectra of the PBSs isolated from *Synechocystis* WT and ΔPB-loop mutant cells are compared in Fig. 4. At the room temperature, both spectra virtually coincide and have the identical PC

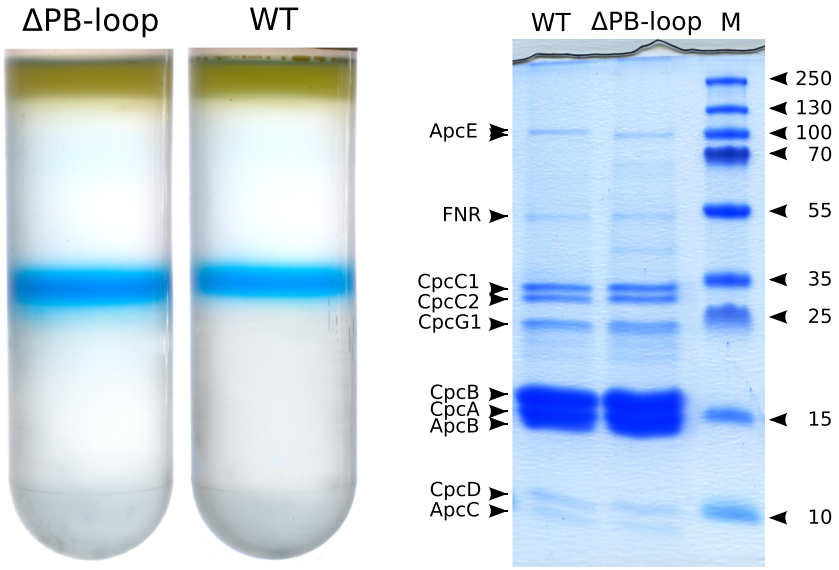

Fig. 3. On the left: the tubes with sucrose density gradient containing PBSs isolated from ΔPB-loop mutant and WT *Synechocystis* after the ultracentrifugation. On the right: polypeptide composition of the PBS-containing zones. Molecular mass markers (M) are indicated in kDa.

absorption peak at 620 nm with the APC shoulder at 650 nm (Fig. 4A). At 77 K, the spectra are characterized by two PC peaks at 595 and 630 nm and the distinct APC shoulder at 650 nm (Fig. 4B). It can be concluded that the mutant PBS does not differ from the WT strain PBS in the absorption properties.

The steady-state fluorescence emission spectra demonstrated no difference between the PBSs from the ΔPB-loop and WT cells (Fig. 5). At the room temperature, the PBS spectrum of the WT *Synechocystis* had one broad unresolved band at 667 nm and a long-wavelength shoulder. The overall shape of the ΔPB-loop PBS spectrum follows the shape of the WT PBS spectrum with a slight blue shift of the main peak position to 665 nm (Fig. 5A). The ratio of the WT and ΔPB-loop PBS fluorescence quantum yields determined as the area under the fluorescence emission curves was equal to 1.05 ± 0.04.

At 77 K, the WT *Synechocystis* PBS spectrum was characterized by a sharp peak at 683 nm corresponding to the long-wavelength emitters. The spectrum of the mutant PBS coincides in shape with the WT-spectrum, but the main peak position is shifted to 682 nm (Fig. 5B). A small hypsochromic shift of the PBS fluorescence maximum was observed earlier in the analogous ΔPB-loop mutant of *Synechocystis* sp. PCC 6714 [40]. Since, the PBS fluorescence at 77 K mainly belongs to the terminal emitter(s), this result indicates that deleting the PB-loop does not distort the internal energy transfer pathways among the phycobilin chromophores in the mutant PBS. Thus, the latter is fully functional from the spectral point of view and the impact of the PB-loop deletion on the PBS architecture is inconspicuous.

3.5. Cell fluorescence spectra

Upon the excitation at 440 nm, at the room temperature, the cell fluorescence emission spectra of both strains are characterized by a single chlorophyll band (683 nm) and are very similar in shape. In both cases, no signs of PBS emission were found. Nevertheless, the fluorescence from the mutant cell samples was more intensive when measured at the equal chlorophyll concentration. According to the under-curve areas ratio, the mutant cells sample has 1.69 ± 0.12 times more intensive emission (Fig. 6A). Given that the fluorescence emission at the room temperature originates predominantly from PSII, this data means that in the mutant cells the portion of PSII in total chlorophyll amount is higher than in the WT *Synechocystis*.

Upon excitation at 580 nm, at the room temperature, the spectrum of WT *Synechocystis* cells is dominated by the phycobiliprotein

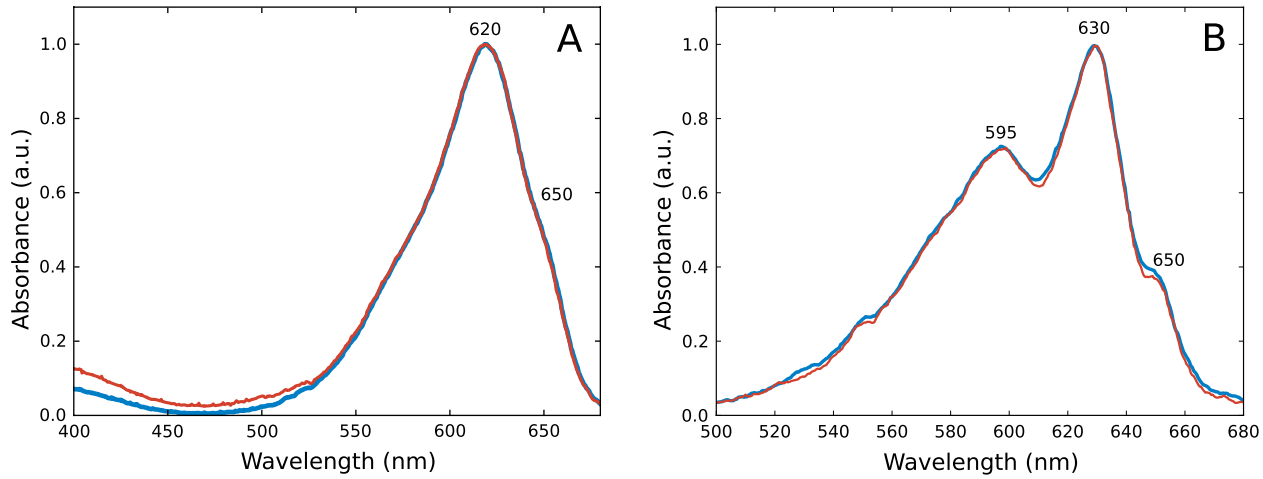

Fig. 4. Absorption spectra of the PBSs isolated from the WT *Synechocystis* (blue) and ΔPB-loop mutant (red) cells at the room temperature (A) and 77 K (B). Spectra were normalized at their main peak positions.

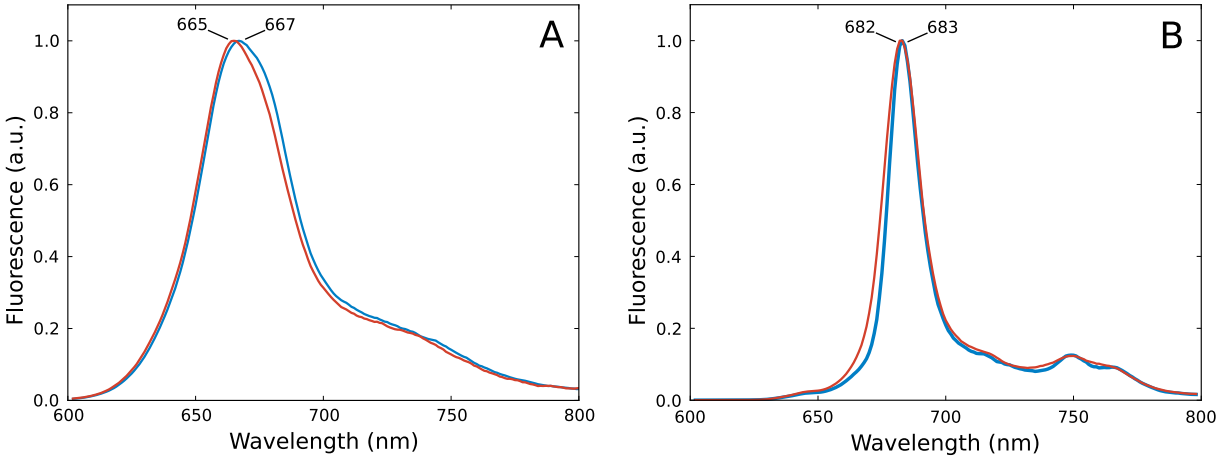

Fig. 5. Fluorescence emission spectra of the PBSs isolated from the *Synechocystis* WT (blue) and ΔPB-loop mutant (red) cells upon excitation at 580 nm at the room temperature (A) and 77 K (B). Spectra were normalized at their main peak positions.

(PC + APC) peak at 657 nm (Fig. 6B). Due to the energy transfer from PBS to chlorophyll, the second band at 683 nm could originate from the PSII chlorophyll and partially from the PBS terminal emitters. The spectrum of the ΔPB-loop cells contains the same two bands yet in a different proportion. When measured for equal PBS as well as chlorophyll amount (see absorption spectra in Fig. 2), the fluorescence intensity of the mutant sample was 1.85 ± 0.15 times higher (Fig. 6B). This data corresponds well to the results of the excitation at 440 nm (Fig. 6A) and indicates that the PBSs in the mutant cells are less effectively coupled with PSII.

Upon the direct excitation of chlorophyll at 440 nm, at 77 K, we observed the ‘ traditional’ fluorescence emission spectrum of the WT *Synechocystis* with two low intensity PSII bands at 685 and 695 nm, as well as the intensive long-wavelength PSI peak at 723 nm [55,56]. The spectrum of the ΔPB-loop mutant exhibited the same three peaks but with a higher relative intensity of the PSII bands at 685 and 695 nm (Fig. 7A). Since, at 77 K there is a quantitative linear relationship between PSII/PSI fluorescence peak intensities and the molar ratio of the photosystems [56], The 1.8 ± 0.1 times higher ratio of the PSII and PSI peak intensities indicates that a higher portion of chlorophyll is provided by PSII in the ΔPB-loop mutant compared to WT *Synechocystis*. Thus, according to the room temperature and 77 K fluorescence spectra measurements (Figs. 6A and 7A, correspondingly) the PSII/PSI ratio is altered in favor of PSII in the mutant. The similar but much more pronounced effect of the PSII relative content increase was observed earlier in response to the reduction of the PC lateral rods [53,54] and whole PBSs [57,58].

Changes in the energy transfer from the mutant PBSs to the chlorophyll can be registered by means of the alteration of the fluorescence emission upon PBS excitation. At the room temperature, it is difficult to infer definite conclusions due to the superfluously broad fluorescence emission bands of the PBS and PSII accompanied by their overlapping (Fig. 6B). Upon the excitation at 580 nm and 77 K, fluorescence emission spectra of WT *Synechocystis* and ΔPB-loop cells differ drastically (Fig. 7B). The spectrum of WT *Synechocystis* is characterized by three band groups repeatedly described in the literature: the short-wavelength PBS bands at 650 and 665 nm; the PSII peaks at 685 and 695 nm in the middle part of the spectrum; and the long-wavelength PSI peak at 724 nm.

The spectrum of the ΔPB-loop mutant has the same short-wavelength bands of the bulk PC and APC presented in the region 650–665 nm as the shoulders. Comparing to the WT *Synechocystis* spectrum (Fig. 7B), the middle band of PSII is narrowed with its peak position blue-shifted from 685 to 682 nm and there is no PSII band at 695 nm. Long-wavelength band is very small with its peak position also blue-shifted from 724 to 721 nm. It could be suspected that these differences arise from the intensive PBS fluorescence in the mutant cells.

We have compared the 77 K fluorescence spectra of both cell strains with the spectrum of the isolated mutant PBS (Fig. 7B). The main peak positions were identical (682 nm) in the ΔPB-loop cells (red) and

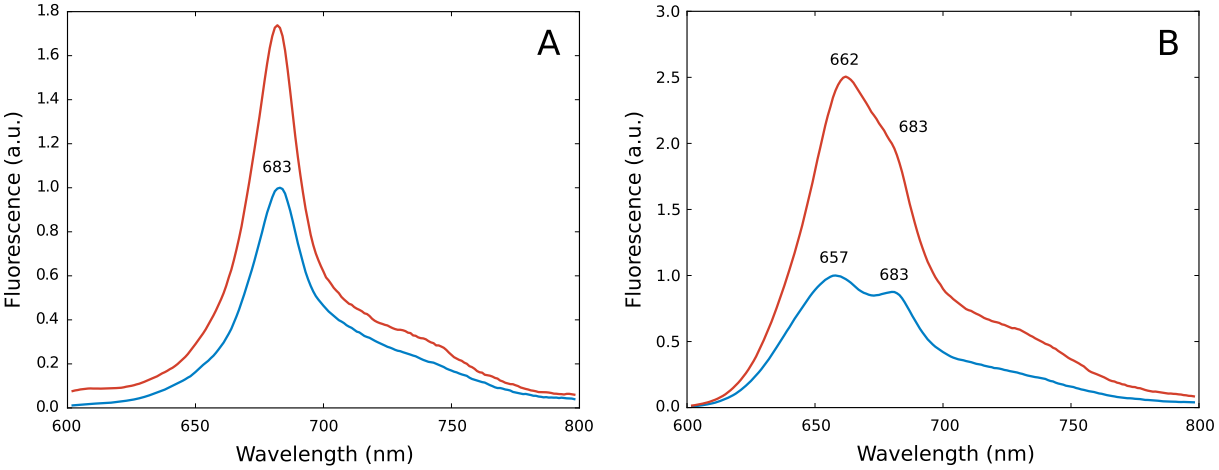

Fig. 6. Room temperature fluorescence emission spectra of the WT *Synechocystis* (blue) and ΔPB-loop mutant (red) cells upon excitation at 440 nm (A) and 580 nm (B). Spectra were recorded for the cell samples equalized by the chlorophyll concentration and normalized on the WT *Synechocystis* spectra main maxima.

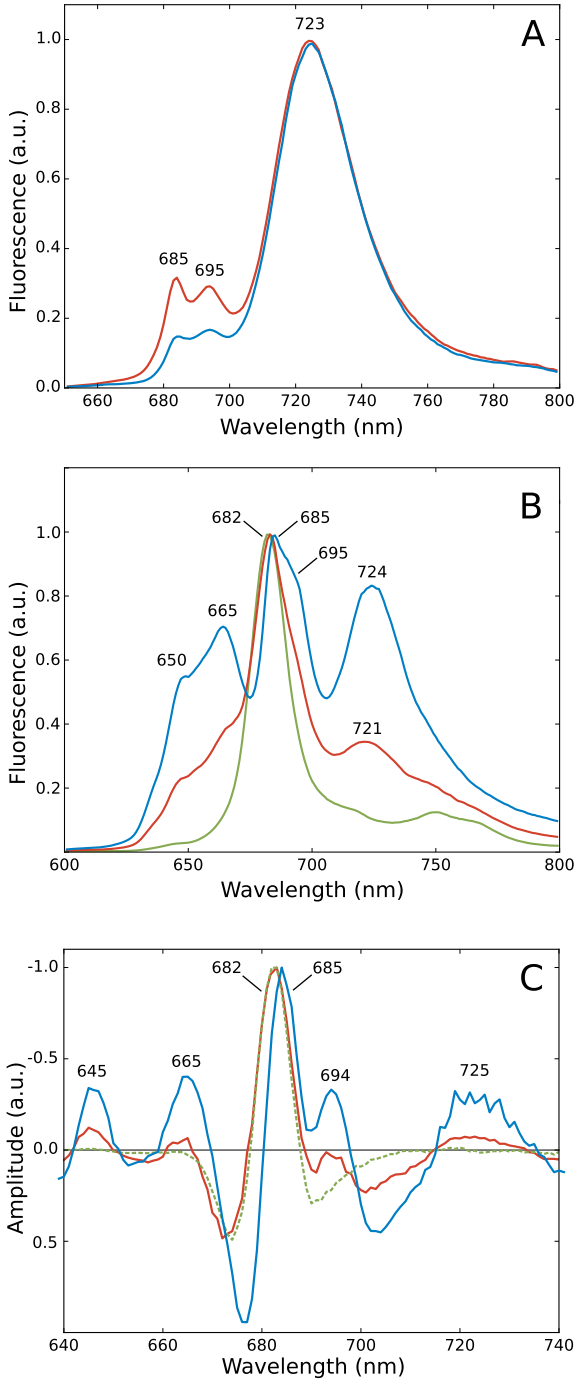

Fig. 7. 77 K fluorescence emission spectra upon excitation at 440 nm (A) and 580 nm (B) of the WT *Synechocystis* (blue) and ΔPB-loop mutant (red) cells. In (B) the spectrum of the isolated mutant PBSs (green) is reproduced from Fig. 5B for comparison. C. The second derivatives of the spectra presented in (B). Spectra were normalized at their main peak positions.

isolated mutant PBSs (green), while in the WT *Synechocystis* cells spectrum, the main peak was present at 685 nm (blue). Therefore, in the ΔPB-loop cells a substantial part of the fluorescence belongs to the flared up emission of PBSs. The same pattern was observed in the second derivatives of the 77 K fluorescence emission spectra: in the spectrum of WT *Synechocystis* the main peak was disposed at 685 nm, while in the spectra of the mutant cells and isolated mutant PBSs it was shifted to 682 nm (Fig. 7C). The domination of the 77 K fluorescence spectrum by the peak of the PBS terminal emitters indicates the disturbance of the energy transfer from PBS to the thylakoid membrane in the ΔPB-loop mutant, although the absorption and fluorescence spectral properties coincided in the isolated WT and ΔPB-loop PBS samples.

3.6. Ultrastructure of the cells

The fluorescent spectral data on the increased PSII/PSI ratio as well as the altered energy migration from PBS to chlorophyll made us verify the thylakoid's arrangement in the ΔPB-loop mutant cells. The WT *Synechocystis* produces spherical cells up to 2 μm in diameter that are well characterized by electron microscopy [59-63]. In our study, the obtained thin sections of the WT *Synechocystis* cells demonstrate numerous thylakoid membranes (usually 5 at the middle phase of the cell growth) running regularly in parallel at the periphery of the cytoplasm, so that the central region is usually devoid of thylakoids. The average distance between the adjacent thylakoid membranes was found to be stable and equal to 45 ± 6 nm. The curvature of the thylakoid membranes correlates with the curvature of the cell envelope (Fig. 8A). These results are typical of *Synechocystis* sp. PCC 6803 [46,59,61,62].

In the ΔPB-loop cells, the intracellular organization of the thylakoid system has changed and the number of the membranes decreased to 3–4 (Fig. 8B and C). Thylakoids were less regular, more curved and did not follow the shape of the cell envelope as in the WT *Synechocystis*. In some cytoplasmic regions, the distance between thylakoid membranes decreased down to ~35 nm, while in the other ones increased up to ~ 75 nm. On the average, the inter-thylakoid distance in the ΔPB-loop mutant cells was 60 ± 20 nm being longer than in the WT cells. The thylakoid membranes were shortened and their curvature was more variable contracted to the WT *Synechocystis*.

The *Synechocystis* is highly amendable to genetic manipulations with PBS. That gave rise to a plethora of variably pigmented strains exhibiting changes in their thylakoid structure in response to PBS alteration [46,59-63]. Along with the WT *Synechocystis* the thylakoid membranes arrangement was described for the range of other cyanobacterial species [64,65]. Cyanobacterial thylakoid membranes are known to be separated by a space sufficient for two zipped rows of PBSs to be placed [66,67]. However, how the complexes of PSII and PSI and their PBS-antenna are assembled in the thylakoids as well as how the organization of these membrane regions could be extrapolated to the whole cell level, is not entirely clear. Nevertheless, the observed morphological changes in the ΔPB-loop cells are definitely related with the decline in the efficiency of PBS and thylakoids coupling.

3.7. Fluorescence induction and state transitions

The PAM fluorimetry technique was used to evaluate the correlation between the changes in the energy transfer from PBS to the thylakoid membrane and the increased relative content of PSII. In PAM measurements, the minimal fluorescence level (F_0) is registered under the non-actinic amplitude-modulated light of a low intensity in the dark-adapted cells. Under the low intensity excitation at 650 nm, all the reaction centers of PSII are open and the fluorescence is emitted both from chlorophyll and PBS [68]. The increased fluorescence level $F_{M'}$ is achieved in actinic light due to the overflowing and closing of the PSII reaction centers. The parameter $F_v/F_{M'} = (F_{M'} - F_0)/F_{M'}$ is generally used as a criterion for the PSII functional activity in higher plants [69], but this assumption does not generally hold for cyanobacteria [68,70], as the variable fluorescence component arises from PSII, while the constant (F_0) component is provided by the emission from both PSII and PBS [71]. The F_0-signal in the WT *Synechocystis* was rather low and, correspondingly, the parameter F_v/F_M was about 0.5 being in the range (0.4–0.6) typical of cyanobacteria [68].

When registered for equal amounts of chlorophyll, the F_0 level was twice as high in the ΔPB-loop sample compared to the WT cells (Fig. 9). A higher F_0 in the ΔPB-loop samples correlates well with the decrease in connectivity between the PBSs and thylakoid membranes, as some amount of the uncoupled PBSs was reported to be a possible reason for

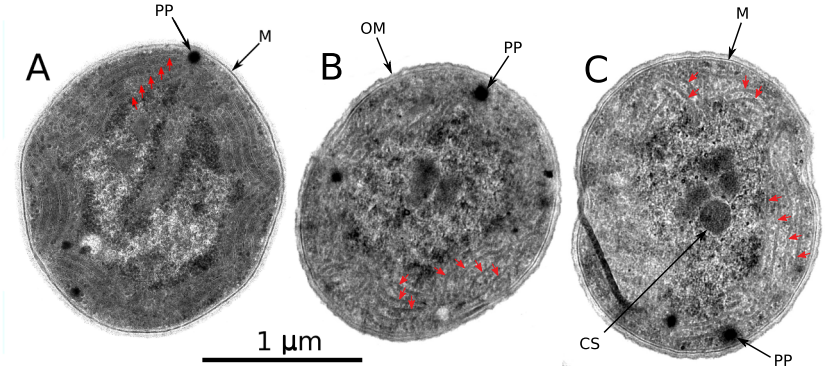

Fig. 8. Thin-section electron micrographs of the WT *Synechocystis* and ΔPB-loop mutant cells. A. The WT cells demonstrate thylakoids having regular curvature and running at the periphery of the cytoplasm. B and C. Cell and semi-dividing cell of the ΔPB-loop mutant with partially destroyed thylakoid membrane system. Letters denote: M — murein, OM — outer membrane, PP — polyphosphate bodies, CS — carboxysomes; red arrows indicate thylakoid membranes.

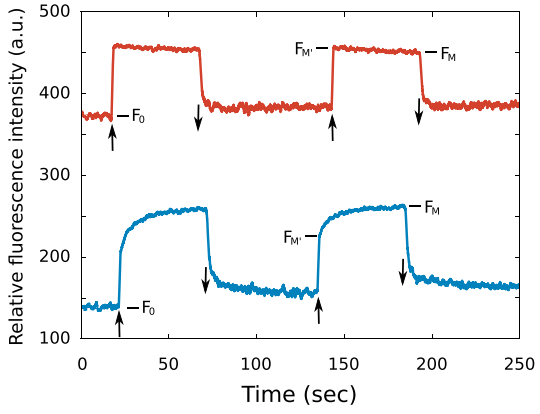

Fig. 9. The fluorescence kinetics of the WT *Synechocystis* (blue) and ΔPB-loop (red) cells measured in a PAM fluorometer. F_0— the minimal fluorescence in 650 nm non-actinic modulated light in presence of DCMU added to the sample after dark adaptation; $F_{M'}$ — the maximal fluorescence under the 580 nm actinic light illumination of the dark adapted cells; F_M— the maximal fluorescence after 50 s of actinic illumination.

F_0 increase in cyanobacteria [72,73]. At the same time, the F_v signal amplitude from two samples was equal (Fig. 9), thus indicating a comparable photosynthetic activity of PSII in two samples when determined per total chlorophyll. Given that the PSII portion is higher in the mutant cells, it looks like some part of the PSII core complexes (probably having disturbed contact with the PBSs) was less effectively coupled to the electron transport chain in the ΔPB-loop mutant. This part of the PSII complexes can also account for the increase of F_0 level. Thus, the increased PSII titer led to the preservation of the proper photosynthetic activity in the mutant cells.

In the WT *Synechocystis* sample, the fluorescence intensity slowly grows from the $F_{M'}$ up to the F_M level in actinic light, while no similar effect was observed in the mutant cells (Fig. 9). In the darkness, the cyanobacterial cells exist in state 2 [68,72], and the signal increase registered in WT cells corresponds to state 2 → state 1 transition induced by the oxidation of the PQ pool upon illumination [72,74-76]. The absence of this effect in the ΔPB-loop cell samples points at a strongly diminished ability of the mutant strain to perform state transitions.

The adaptation to either state 1 or state 2 can also be revealed by the fluorescence emission spectra registered after fixing the corresponding state by freezing the cells in liquid nitrogen [72,77,50]. In state 1, the relative intensity of the fluorescence emission from PSII is greater than in the cells adapted to state 2 [64,72]. The 77 K fluorescence emission spectra of the dark- and light-adapted WT *Synechocystis* cells clearly indicate the transition from state 2 to state 1, as the relative amplitude of the PSII fluorescence bands at 685 and 695 nm grew in respect to PSI fluorescence peak at 725 nm (Fig. 10A). At the same time, the corresponding spectra of the mutant cells are nearly the same (Fig. 10B), that illuminates diminished ability of the mutant to perform state transitions [72,75] and corresponds well to the PAM data.

3.8. OCP-dependent PBS quenching

The transition from state 2 to state 1 occurs under a relatively low light intensity, while the illumination of the cyanobacterial cells by the strong blue-green light induces the non-photochemical PBS quenching. The latter is triggered by the $OCP^O \rightarrow OCP^R$ phototransformation [33]. In accordance with all the earlier observations [33,36], blue-green light induced the significant (47 ± 7 %) decrease of the PBS fluorescence in the WT *Synechocystis* (Fig. 11A). In contrast, the quenching in the ΔPB-loop mutant cells (Fig. 11B) was two times lower (26 ± 11 %).

In cyanobacteria, the quenching of PBS fluorescence is provided by only one OCP molecule attaching to the whole PBS [78]. Therefore, the OCP binding site should be located close to the terminal emitter chromophore that collects energy from all the other phycobilins of the PBS [25,79,80]. Compared to the bulk APC's chromophores, the chromophore of ApcE is shifted towards the protein surface that should diminish the distance to the carotenoid chromophore of OCP [23-25]. Thus, the revealed decrease of the OCP-induced PBS quenching in the mutant indicates that the PB-loop participates in the PBS and OCP interaction.

3.9. Oxygen photoevolution

The measurement of the oxygen photoevolution rate allows to evaluate the effect of deleting the PB-loop on the photosynthetic activity of *Synechocystis*. Upon excitation at 440 nm, the rate of oxygen photoevolution was the same in the WT and ΔPB-loop cell samples with equal chlorophyll concentrations (Table 1, Fig. S3A). Thus, the WT and mutant cells demonstrate equal PSII activity. The analogous match was obtained when oxygen photoevolution was registered in the 590 nm light absorbed by PBS (Table 1, Fig. S3B). Besides, the ΔPB-loop strain demonstrates an increased rate of oxygen consumption than the WT *Synechocystis* (Table 1, Fig. S3) getting balanced physiological response to the mutation [81].

At the first glance, this result does not correlate with the 77 K cell fluorescence emission spectra that demonstrate the increased 1.7–1.8 times PSII to PSI ratio in the ΔPB-loop strain (Fig. 7A). Nevertheless, all the polarographic measurements were made at least in triplicate and the results were reproducible. Thus, we have to conclude that in the mutant cells the overall activity of the linear electron transport chain decreased.

In general, the PBS truncation brings about the increase of PSII titer in various *Synechocystis* mutants [53,54,57,58,82]. The degree of this effect in case of the ΔPB-loop cells is precisely sufficient to compensate for the physiological consequences of the decreased PSII activity. This provides for the equal growth rate of the ΔPB-loop and WT *Synechocystis* sp. PCC 6803 and 6714 [12] strains and explains the increased PSII/PSI ratio.

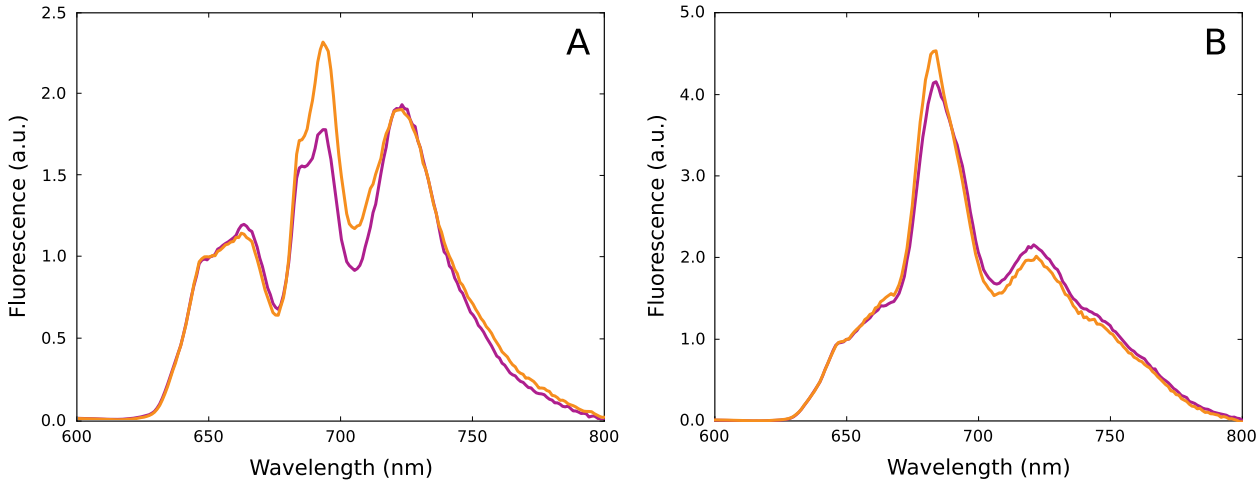

Fig. 10. The 77 K fluorescence emission spectra (excitation at 580 nm) of the WT *Synechocystis* (A) and ΔPB-loop mutant (B) strain cells in the dark- (violet) and light-adapted (orange) states. The spectra were normalized at the PC emission maximum (650 nm).

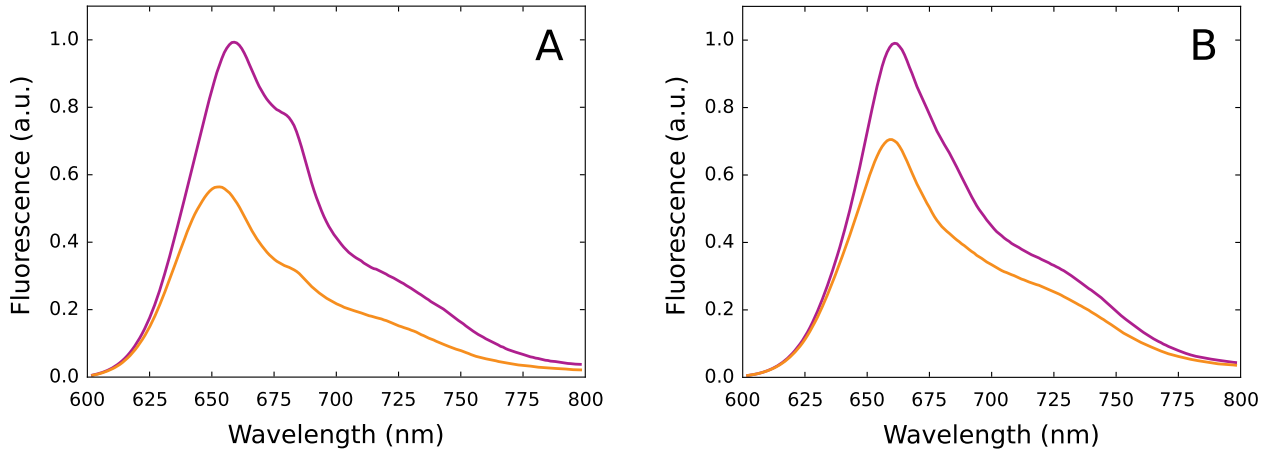

Fig. 11. The room temperature fluorescence emission spectra (excitation at 580 nm) of the WT *Synechocystis* (A) and ΔPB-loop mutant (B) cells adapted to the dark (violet) or preilluminated by intense blue-green light (orange) activating $OCP^O \rightarrow OCP^R$ photoconversion. Spectra were measured for equal PBS concentrations to avoid any difference in light reabsorption by the samples.

3.10. P700 photooxidation

In the equalized by chlorophyll content samples, under the excitation both at 620 nm (PBS) and 730 nm (PSI), the level of the $P700^+$ signal was higher in the WT *Synechocystis* corresponding to the higher PSI/PSII ratio compared to the mutant (Fig. 12). Based on the P700 photooxidation kinetics (Fig. S4) and known for cyanobateria share of the PSII chlorophyll (equal to 5–10 % of the total pigment [71]), the relative PSI content in the mutant cells would be 88 ± 3 % of that in the WT *Synechocystis*. This result quantitatively corresponds to the obtained data on the 1.8 ± 0.1 times higher content of PSII in the mutant (Fig. 7A).

Table 1
Rates of the WT *Synechocystis* (WT) and ΔPB-loop mutant (LM) strains photoevolution (μmol O_2 per mg Chl per hour) under 440 and 590 nm excitation light (160 and 140 μmol m^{-2} s^{-1}, respectively) and oxygen consumption in the dark. The samples were equalized by chlorophyll content.

	O_2 photoevolution		O_2 consumption darkness
	440 nm	590 nm	
WT	12.1 ± 4.2	45.1 ± 1.8	$(1.6 \pm 0.2) \cdot 10^{-2}$
LM	12.9 ± 1.2	43.1 ± 4.7	$(2.1 \pm 0.2) \cdot 10^{-2}$

The rate constant of P700 photooxidation can be estimated based on the dependence of the equilibrium $P700^+$ level on the illumination intensity (Fig. S4) and the $P700^+$ reduction rate constants (see Appendix for derivation and Table 2). The rate constants of the P700 photooxidation were found to be approximately equal for the WT and ΔPB-loop strains under the PBS as well as PSI specific light (Table 2). Since no difference was revealed in the P700 photooxidation constants, there is no effect of the PB-loop deletion on the energy transfer from PBS to PSI.

There are two independent terminal energy emitters in the PBS core (ApcE and ApcD [1,5,83]) that collect energy from the bulk APCs and are located in the different APC trimers of PBS core basal cylinders [27,84]. ApcD is known to mediate energy transfer from the PBS to PSI [76,85,86]. Thus, one of the possible causes for preservation of energy transfer from PBS to the chlorophyll in the ΔPB-loop mutant is the absence of any effect of this mutation on the ApcD terminal emitter. Furthermore, the cytoplasmic surface of the PSII dimer is flat and there are two cavities on this surface located exactly in front of the PB-loop sites on the PBS bottom surface [13,87]. Thus, it looks reasonable that PB-loop participates in the PBS and PSII interaction. On the contrary, the cytoplasmic surface of the PSI possesses a large protrusion formed by three polypeptides (PsaC, PsaD, and PsaE) that ideally fits the furrow between the basal cylinders of the PBS core [15]. Thus, the PB-loop should give lower contribution to PBS and PSI interaction.

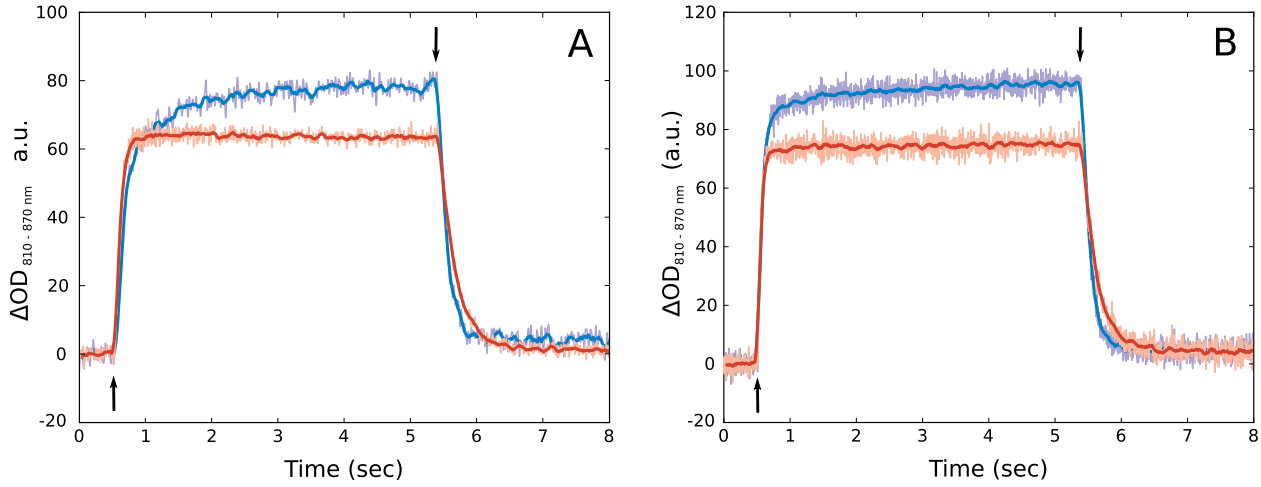

Fig. 12. The kinetics of P700 photooxidation in the WT *Synechcocystis* (blue) and ΔPB-loop mutant (red) cells pre-incubated for 15 min in the dark. The arrows indicate light switched on (↑) and off (↓). The P700 redox state changes were induced by 730 nm (A) and 620 nm (B) actinic light illumination (1800 and 400 μmol $m^{-2} s^{-1}$, respectively).

Table 2
Effective rate constants (see Appendix) of P700 photooxidation (k_1) under excitation light absorbed by PSI (730 nm) and PBSs (620 nm), and the rate constants of $P700^+$ reduction in the dark (k_2). The data is demonstrated for WT *Synechocystis* (WT) and ΔPB-loop mutant (LM).

	730 nm		620 nm	
	k_1 (m^2 μmol^{-1})	k_2 (s^{-1})	k_1 (m^2 μmol^{-1})	k_2 (s^{-1})
WT	$(1.7 \pm 0.8)10^{-5}$	$(7.2 \pm 0.8)10^{-3}$	$(1.5 \pm 0.3)10^{-4}$	$(7.6 \pm 0.3)10^{-3}$
LM	$(2.0 \pm 0.5)10^{-5}$	$(4.2 \pm 0.5)10^{-3}$	$(1.8 \pm 0.6)10^{-4}$	$(4.0 \pm 0.7)10^{-3}$

Upon the excitation light of low intensity the WT *Synechocystis* demonstrated a rather slow increase of the $P700^+$ level, compared to the mutant (Fig. 12). The timescale of the observed effect was in the range of several seconds and became most prominent under the 730 nm excitation light. Long dark preadaptation (15 min in our case) is known to cause the decrease of the $P700^+$ accumulation rate in the WT *Synechocystis* [81]. As incubation of the cyanobacterial cells in the dark induces state 2 [68,72], the slowdown of the $P700^+$ kinetics after the dark adaptation could be accounted by the transition to state 1. Since this effect was not observed and the P700 photooxidation kinetics was remarkably faster in the ΔPB-loop samples, it looks like the mutant cells always exist in state 1. This proposition correlates with the observed deficiency of the PSII functioning in the mutant cells that should cause partial oxidation of the PQ pool and, therefore, transition to state 1.

4. Conclusion

The obtained data shed light on the functional role of the PB-loop in PBS. The PBSs in the ΔPB-loop cells were successfully assembled and the polypeptide compositions of the WT and mutant PBSs were identical except the small difference in the ApcE masses. The internal energy transfer pathways among the bulk phycobilin chromophores and terminal emitters were not affected in the ΔPB-loop PBSs. This result correlates well with the external PB-loop location on the bottom PBS surface [23,25] and corresponds to the earlier speculations implying that the PB-loop is exposed on the PBS core surface towards the thylakoid membrane [6,9]. However, the observed decrease of the PBS and PSII coupling in the ΔPB-loop cells implies that the PB-domain not only transfers energy to the photosynthetic reaction centers, but also participates in PBS anchoring to the PSII complexes. That is why, in response to the PB-loop deletion, the content of the PSII was increased in the mutant cells. This allowed to compensate the partial loss of PSII energy supply as follows from the oxygen evolution and fluorescence PAM measurements.

There were two uncompensated consequences of the PB-loop deletion concerning short term light adaptations. First was a disturbance of the state transitions due to the diminishing of PBS and PSII coupling. The second was a two-fold decrease of the OCP-dependent PBS fluorescence quenching. Both effects are related to the protein-protein interaction between the PBS and other photosynthetic proteins. In general, the protein-protein interactions are promoted by the hydrophobic forces, and the PB-loop comprises a lot of hydrophobic residues [24]. Therefore, the PB-loop most probably participates in the attachment of PBS to the PSII complex and OCP. Nevertheless, a complete understanding of molecular details of PBS interaction with the thylakoid membranes and OCP needs additional in depth investigations.

Transparency document

The Transparency document associated with this article can be found, in online version. Supplementary data to this article can be found online at https://doi.org/10.1016/j.bbabio.2018.10.004.

Acknowledgments

The authors are indebted to Prof. Nikolai B. Gusev and Dr. Sci. Mahir D. Mamedov for supporting, comments and fruitful discussion.

Appendix A

The P700 photocycle could be described as a simple first-order reaction:

$$P700 \underset{k_2}{\overset{k_1 I}{\rightleftharpoons}} P700^+$$

where k_1– is the effective first-order photooxidation rate constant, k_2 — is an effective first-order $P700^+$ reduction rate constant, and I — is a light intensity. When light is on the solution for this scheme would be:

$$[P700^+]_{light\ on} = \frac{k_1 I}{k_1 I + k_2} P_0 (1 - e^{-(k_1 I + k_2)t}),$$

where P_0 — is a signal level when all the PSI reasction center were oxidized. When the light is on for some sufficient time period, the $P700^+$ signal level would achieve the equilibrium level of

$$P_{eq} = \frac{k_1 I}{k_1 I + k_2} P_0$$

and after light switching off, the $P700^+$ state would reduce with the rate constant k_2:

$$[P700^+]_{light\ off} = \frac{k_1 I}{k_1 I + k_2} P_0\, e^{-k_2 t}$$

here I — is a light intensity before switching off. Thus, the values for k_2 can be obtained directly from the experimental curves (Fig. S4) via fitting procedure. The P_0 and P_{eq} levels are also available from the experiment. So, the rate constant k_1 describing the rate of energy flow to PSI can be obtained based on the P_{eq}, P_0, k_2, and corresponding I:

$$k_1 = \frac{k_2}{I}\left(\frac{P_{eq}}{P_0 - P_{eq}}\right).$$

Appendix B. Supplementary data

Supplementary data to this article can be found online at https://doi.org/10.1016/j.bbabio.2018.10.004.

References

[1] W.A. Sidler, Phycobilisome and phycobiliprotein structures, in: D.A. Bryant (Ed.), The Molecular Biology of Cyanobacteria, Springer, Netherlands, 1994, pp. 139–216.
[2] L.-N. Liu, X.-L. Chen, Y.-Z. Zhang, B.-C. Zhou, Characterization, structure and function of linker polypeptides in phycobilisomes of cyanobacterria and red algae, Biochim. Biophys. Acta 1708 (2005) 133–142.
[3] N. Adir, Elucidation of the molecular structures of components of the phycobilisome: reconstructing a giant, Photosynth. Res. 85 (2005) 15–32.
[4] M. Watanabe, M. Ikeuchi, Phycobilisome: architecture of a light-harvesting supercomplex, Photosynth. Res. 116 (2013) 265–276.
[5] D.A. Bryant, D.P. Canniffe, How nature designs light-harvesting antenna systems: design principles and functional realization in chlorophototrophic prokaryotes, J. Phys. B Atomic Mol. Phys. 51 (2018) 033001.
[6] A.N. Glazer, Phycobilisome: a macromolecular complex optimized for light energy transfer, Biochim. Biophys. Acta 768 (1984) 29–51.
[7] W. Reuter, G. Wiegand, R. Huber, M. Than, Structural analysis at 2.2 Å of orthorhombic crystals presents the asymmetry of the allophycocyanin-linker complex, AP·$L_C^{7.8}$ from phycobilisomes of *Mastigocladus laminosus*, Proc. Natl. Acad. Sci. USA 96 (1999) 1363–1368.
[8] D.J. Lundell, A.N. Glazer, Allophycocyanin B, J. Biol. Chem. 256 (1981) 12600–12606.
[9] D.J. Lundell, A.N. Glazer, Molecular architecture of a light-harvesting antenna. Core substructure in *Synechococcus* 6301 phycobilisomes: two new allophycocyanin and allophycocyanin B complexes, J. Biol. Chem. 258 (1983) 902–908.
[10] V. Capuano, A.-S. Braux, N.T. de Marsac, J. Houmard, The "Anchor Polypeptide" of cyanobacterial phycobilisomes. Molecular characterisation of the *Synechococcus* sp. PCC 6301 *apcE* gene, J. Biol. Chem. 266 (1991) 7239–7247.
[11] D.A. Bryant, R. de Lorimier, G. Guglielmi, S.E.S. Jr, Structural and compositional analyses of the phycobilisomes of *Synechococcus* sp. PCC 7002. Analyses of the wild-type strain and a phycocyanin-less mutant constructed by interposon mutagenesis, Arch. Microbiol. 153 (1990) 550–560.
[12] A.A. Arteni, G. Ajlani, E.J. Boekema, Structural organization of phycobilisomes from *Synechocystis* strain PCC 6803 and their interaction with the membrane, Biochim. Biophys. Acta 1787 (2009) 272–279.
[13] L. Chang, X. Liu, Y. Li, C. Liu, F. Yang, J. Zhao, S.F. Sui, Structural organization of an intact phycobilisome and its association with photosystem II, Cell Res. 25 (2015) 726–737.
[14] J. Zhang, J. Ma, D. Liu, S. Qin, S. Sun, J. Zhao, S.-F. Sui, Structure of phycobilisome from the red alga *Griffithsia pacifica*, Nature 551 (2017) 57–63.
[15] D.V. Zlenko, T.V. Galochkina, P.M. Krasilnikov, I.N. Stadnichuk, Coupled rows of PBS cores and PSII dimers in cyanobacteria: symmetry and structure, Photosynth. Res. 133 (2017) 245–260.
[16] B.A. Zilinskas, L.S. Greenwald, Isolation and characterization of the central component of the phycobilisome core of *Nostoc* sp. plant Physiol. 70 (1982) 1060–1065.
[17] M. Mimuro, E. Gantt, A high molecular weight terminal pigment ("Anchor Polypeptide") and a minor blue polypeptide from phycobilisomes of the cyanobacterium *Nostoc* sp. (MAC): isolation and characterization, Photosynth. Res. 10 (1986) 201–208.
[18] K.-H. Zhao, P. Su, S. Böhm, B. Song, M. Zhou, C. Bubenzer, H. Scheer, Reconstitution of phycobilisome core-membrane linker, L_{CM}, by autocatalytic chromophore binding to ApcE, Biochim. Biophys. Acta 1706 (2005) 81–87.
[19] I.N. Stadnichuk, M.F. Yanyushin, E.G. Maksimov, E.P. Lukashev, S.K. Zharmukhamedov, I.V. Elanskaya, V.Z. Paschenko, Site of non-photochemical quenching of the phycobilisome by orange carotenoid protein in the cyanobacterium *Synechocystis* sp. PCC 6803, Biochim. Biophys. Acta 1817 (8) (2012) 1436–1445.
[20] D.A. Bryant, Phycobilisomes of *Synchechococcus* sp. RCC 7002 *Pseudanabaena*, in: H. Scheer, S. Schneider (Eds.), Photosynthetic Light-harvesting Systems: Organization and Function, W. de Gryter & Co., New York, 1988, pp. 217–232.
[21] J. Houmard, V. Capuano, M. Colombano, T. Coursin, N.T. de Marsac, Molecular characterization of the terminal energy acceptor of cyanobacterial phycobilisomes, Proc. Natl. Acad. Sci. USA 87 (1990) 2152–2156.
[22] V. Capuano, J.-C. Thomas, N.T. de Marsac, J. Houmard, An *in vivo* approach to define the role of the L_{CM}, the key polypeptide of cyanobacterial phycobilisomes, J. Biol. Chem. 268 (1993) 8277–8283.
[23] X. Gao, T.-D. Wei, N. Zhang, B.-B. Xie, H.-N. Su, X.-Y. Zhang, X.-L. Chen, B.-C. Zhou, Z.-X. Wang, J.-W. Wu, Y.-Z. Zhang, Molecular insights into the terminal energy acceptor in cyanobacterial phycobilisome, Mol. Microbiol. 85 (2012) 907–915.
[24] K. Tang, W.-L. Ding, A. Höppner, C. Zhao, L. Zhang, Y. Hontani, J.T. Kennis, W. Gärtner, H. Scheer, M. Zhou, K.H. Zhao, The terminal phycobilisome emitter, L_{CM}: a light-harvesting pigment with a phytochrome chromophore, Proc. Nat. Acad. Sci. USA 112 (2015) 15880–15885.
[25] D.V. Zlenko, P.M. Krasilnikov, I.N. Stadnichuk, Role of inter-domain cavity in the attachment of the orange carotenoid protein to the phycobilisome core and to the fluorescence recovery protein, J. Biomol. Struct. Dyn. 34 (2016) 486–496.
[26] J.C. Gingrich, D.J. Lundell, A.N. Glazer, Core substructure in cyanobacterial phycobilisomes, J. Cell. Biochem. 22 (1983) 1–14.
[27] L.K. Anderson, F.A. Eiserling, Asymmetrical core structure in phycobilisomes of the cyanobacterium *Synechocystis* 6701, J. Mol. Biol. 191 (1986) 441–451.
[28] D. Bald, J. Kruip, M. Rögner, Supramolecular architecture of cyanobacterial thylakoid membranes: how is the phycobilisome connected with the photosystems? Photosynth. Res. 49 (1996) 103–118.
[29] T. Redlinger, E. Gantt, A Mr 95,000 polypeptide in *Porphyridium cruentum* phycobilisomes and thylakoids: possible function in linkage of phycobilisomes to thylakoids and in energy transfer, Proc. Natl. Acad. Sci. USA 79 (1982) 5542–5546.
[30] M. Rusckowski, B.A. Zilinskas, Allophycocyanin I and the 95 kDa polypeptide. The bridge between phycobilisomes and membranes, Plant Physiol. 70 (1982) 1055–1059.
[31] A.N. Glazer, Adaptive variations in phycobilisome structure, Adv. Mol. Cell. Biol. 10 (1994) 119–149.
[32] A.V. Ruban, The Photosynthetic Membrane: Molecular Mechanisms and Biophysics of Light Harvesting, John Wiley & Sons, London, UK, 2013.
[33] C.A. Kerfeld, M.R. Melnicki, M. Sutter, M.A. Dominguez-Martin, Structure, function and evolution of the cyanobacterial orange carotenoid protein and its homologs, New Phytologist. 215 (2017) 937–951.
[34] H. Zhang, H. Liu, D.M. Niedzwiedzki, M. Prado, J. Jiang, M.L. Gross, R.E. Blankenship, Molecular mechanism of photoactivation and structural location of the cyanobacterial orange carotenoid protein, Biochem. 53 (2014) 13–19.
[35] D. Harris, O. Tal, D. Jallet, A. Wilson, D. Kirilovsky, N. Adir, Orange carotenoid protein burrows into the phycobilisome to provide photoprotection, Proc. Nat. Acad. Sci. USA 113 (2016) E1655–E1662.
[36] D. Kirilovsky, Modulating energy arriving at photochemical reaction centers: orange carotenoid protein-related photoprotection and state transitions, Photosynth. Res. 126 (2015) 3–17.
[37] D.A. Bryant, Cyanobacterial phycobilisomes: progress towards complete structural and functional analysis via molecular genetics, in: L. Bogorad, I. Vasil (Eds.), Cell Culture and Somatic Cell Genetics of Plants, Academic Press, San Diego, 1991, pp. 257–300.

[38] G. Shen, S. Boussiba, W. Vermaas, *Synechocystis* sp. pcc 6803 strains lacking photosystem i and phycobilisome function, Plant Cell 5 (1993) 1853–1863.
[39] G. Ajlani, C. Vernotte, L. DiMagno, D. Haselkorn, Phycobilisome core mutants of *Synechocystis* PCC 6803, Biochim. Biophys. Acta 1231 (1995) 189–196.
[40] G. Ajlani, C. Vernotte, Deletion of the PB-loop in the L_{CM} subunit does not affect phycobilisome assembly or energy transfer functions in the cyanobacterium *Synechocystis* PCC 6714, Eur. J. Biochem. 257 (1998) 154–159.
[41] Y.M. Gindt, J. Zhou, D. Bryant, K. Sauer, Core mutations of *Synechococcus* sp. PCC 7002 phycobilisomes: a spectroscopic study, J. Photochem. Photobiol. B: Biol. 15 (1992) 75–89.
[42] Y.M. Gindt, J. Zhou, D. Bryant, K. Sauer, Spectroscopic studies of phycobilisome subcore preparations lacking key core chromophores: assignment of excited state energies to the L_{CM}, β^{18} and α^{β} chromophores, Biochim. Biophys. Acta 1186 (1994) 153–162.
[43] P. Maxson, K. Sauer, J. Zhou, D.A. Bryant, A.N. Glazer, Spectroscopic studies of cyanobacterial phycobilisomes lacking core polypeptides, Biochim. Biophys. Acta 977 (1989) 40–51.
[44] D. Jallet, M. Gwizdala, D. Kirilovsky, ApcD, ApcF and ApcE are not required for the orange carotenoid protein related phycobilisome fluorescence quenching in the cyanobacterium *Synechocystis* PCC 6803, Biochim. Biophys. Acta 1817 (2012) 1418–1427.
[45] M.-Y. Ho, N.T. Soulier, D.P. Canniffe, G. Shen, D.A. Bryant, Light regulation of pigment and photosystem biosynthesis in cyanobacteria, Curr. Opin. Plant Biol. 37 (2017) 24–33.
[46] I.V. Elanskaya, D.V. Zlenko, E.P. Lukashev, N.E. Suzina, I.A. Kononova, I.N. Stadnichuk, Phycobilisomes from the mutant cyanobacterium *Synechocystis* sp. PCC 6803 missing chromophore domain of ApcE, Biochim. Biophys. Acta 1859 (2018) 280–291.
[47] A.N. Glazer, Phycobilisomes, Meth. Enzymol. 167 (1988) 304–312.
[48] S.R. Haider, H.J. Reid, B.L. Sharp, Tricine-SDS-PAGE, Meth. Mol. Biol. 869 (2012) 81–91.
[49] H.K. Lichtenthaler, Chlorophylls and carotenoids: pigments of photosynthetic biomembranes, Meth. Enzimol. 481 (1987) 350–382.
[50] I.N. Stadnichuk, E.P. Lukashev, I.V. Elanskaya, Fluorescence changes accompanying short-term light adaptations in photosystem I and photosystem II of the cyanobacterium *Synechocystis* sp. PCC 6803 and phycobiliprotein-impaired mutants: state 1/state 2 transitions and carotenoid-induced quenching of phycobilisomes, Photosynth. Res. 99 (2009) 227–241.
[51] U. Schreiber, C. Klughammer, C. Neubauer, Measuring P700 absorbance changes around 830 nm with a new type of pulse modulation system, Z. Naturforsch 43c (1988) 686–698.
[52] E. Reynolds, The use of lead citrate at high pH as an electron opaque stain in electron microscopy, J. Cell. Biol. 17 (1963) 1055–1059.
[53] G. Bernát, N. Waschewski, M. Rögner, Towards efficient hydrogen production: the impact of antenna size and external factors on electron transport dynamics in *Synechocystis* PCC 6803, Photosynth. Res. 99 (2009) 205–216.
[54] J.-H. Kwon, G. Bernát, H. Wagner, M. Rögner, S. Rexroth, Reduced light-harvesting antenna: consequences on cyanobacterial metabolism and photosynthetic productivity, Algal Res. 2 (2013) 188–195.
[55] D. Fork, P. Mohanty, Light Emission by Plants and Bacteria, Academic Press, New York, USA, 1986.
[56] A. Murakami, Quantitative analysis of 77 K fluorescence emission spectra in *Synechocystis* sp. PCC 6714 and *Chlamydomonas reinhardtii* with variable PS I/PS II stoichiometries, Photosynth. Res. 53 (1997) 141–148.
[57] I.N. Stadnichuk, E.P. Lukashev, I.V. Elanskaya, V.A. Boichenko, N.G. Bukhov, Increase in the rate of photosynthetic linear electron transport in cyanobacteruim *Synechocystis* sp. PCC 6803 lacking phycobilisomes, Rus. J. Plant Physiol. 56 (2009) 439–444.
[58] A. Nagarajan, L.E. Page, M. Liberton, H.B. Pakrasi, Consequences of decreased light harvesting capability on photosystem II function in *Synechocystis* sp. PCC 6803. Life 4 (2014) 903–914.
[59] J. Olive, G. Ajlani, C. Astier, M. Recouvreur, C. Vernotte, Ultrastructure and light adaptation of phycobilisome mutants of *Synechocystis* PCC 6803, Biochim. Biophys. Acta 1319 (1997) 275–282.
[60] M. Liberton, R.H. Berg, J. Heuser, R. Roth, H.B. Pakrasi, Ultrastructure of the membrane systems in the unicellular cyanobacterium *Synechocystis* sp. strain PCC 6803, Protoplasma 227 (2006) 129–138.
[61] A.M. van de Meene, M.F. Hohmann-Marriott, W.F. Vermaas, R.W. Roberson, The three-dimensional structure of the cyanobacterium *Synechocystis* sp. PCC 6803, Arch. Microbiol. 184 (2006) 259–270.
[62] A.M. Collins, M. Liberton, H.D. Jones, O.F. Garcia, H.B. Pakrasi, J.A. Timlin, Photosynthetic pigment localization and thylakoid membrane morphology are altered in *Synechocystis* 6803 phycobilisome mutants, Plant Physiol. 158 (2012) 1600–1609.
[63] D.J. Lea-Smith, P. Bombelli, J.S. Dennis, S.A. Scott, A.G. Smith, C.J. Howe, Phycobilisome-deficient strains of *Synechocystis* sp. PCC 6803 have reduced size and require carbon-limiting conditions to exhibit enhanced productivity, Plant Physiol. 165 (2014) 705–714.
[64] J. Olive, I. M'Bina, C. Vernotte, C. Astier, F. Wollman, Randomization of the EF particles in thylakoid membranes of *Synechocystis* 6714 upon transition from state I to state II, FEBS Lett. 208 (1986) 203–212.
[65] R. Nevo, S.G. Chuartzman, O. Tsabari, Z. Reich, D. Charuvi, E. Shimoni, Architecture of thylakoid membrane networks, in: H. Wada, N. Murata (Eds.), Lipids in Photosynthesis: Essential and Regulatory Functions, Springer Science and Business Media, Dordrecht, The Netherlands, 2009, pp. 295–328.
[66] E. Mörschel, K. Mühlethaler, On the linkage of exoplasmatic freeze-fracture particles to phycobilisomes, Planta 158 (1983) 451–457.
[67] L.K. Anderson, C.M. Toole, A model for early events in the assembly pathway of cyanobacterial phycobilisomes, Mol. Microbiol. 30 (1998) 467–474.
[68] D. Campbell, V. Hurry, A.K. Clarke, P. Gustafsson, G. Öquist, Chlorophyll fluorescence analysis of cyanobacterial photosynthesis and acclimation, Microbiol. Mol. Biol. Rev. 62 (1998) 667–683.
[69] M. Kitajima, W. Butler, Quenching of chlorophyll fluorescence and primary photochemistry in chloroplasts by dibromothymoquinone, Biochim. Biophys. Acta 376 (1975) 105–115.
[70] C. Büchel, C. Wilhem, *In vivo* analysis of slow chlorophyll fluorescence induction kinetics in algae: progress, problems and perspectives, Photochem. Photobiol. B. Biol. 58 (1993) 137–148.
[71] G.C. Papageorgiou, The photosynthesis of cyanobacteria (blue bacteria) from the perspective of signal analysis of chlorophyll a fluorescence, J. Sci. Ind. Res. 55 (1996) 596–617.
[72] C.W. Mullineaux, J.F. Allen, State 1–State 2 transitions in the cyanobacterium *Synechococcus* 6301 are controlled by the RedOx state of electron carriers between photosystems I and II, Photosynth. Res. 23 (1990) 297–311.
[73] D.L. Goosney, A.G. Miller, High rates of O_2 photoreduction by the unicellular cyanobacterium *Synechocystis* PCC 6803 as determined by the quenching of chlorophyll fluorescence, Canad. J. Bot. 75 (1997) 394–401.
[74] P.C. Meunier, M.S. Colón-Lopez, L.A. Sherman, Temporal changes in state transitions and photosystem organization in the unicellular, diazotrophic cyanobacterium *Cyanothece* sp. ATCC 51142, Plant Physiol. 115 (1997) 991–1000.
[75] C. Huang, X. Yuan, J. Zhao, D.A. Bryant, Kinetic analyses of state transitions of the cyanobacterium *Synechococcus* sp. PCC 7002 and its mutant strains impaired in electron transport, Biochim. Biophys. Acta 1607 (2003) 121–130.
[76] C. Dong, A. Tang, J. Zhao, C.W. Mullineaux, G. Shen, D.A. Bryant, ApcD is necessary for efficient energy transfer from phycobilisomes to photosystem I and helps to prevent photoinhibition in the cyanobacterium *Synechococcus* sp. PCC 7002, Biochim. Biophys. Acta 1787 (2009) 1122–1128.
[77] C. Vernotte, C. Astier, J. Olive, State 1–state 2 adaptation in the cyanobacteria *Synechocystis* PCC 6714 wild type and *Synechocystis* PCC 6803 wild type and phycocyanin-less mutant, Photosynth. Res. 26 (1990) 203–212.
[78] M. Gwizdala, A. Wilson, D. Kirilovsky, *In vitro* reconstitution of the cyanobacterial photoprotective mechanism mediated by the orange carotenoid protein in *synechocystis* pcc 6803, Plant Cell 23 (2011) 2631–2643.
[79] I.N. Stadnichuk, M.F. Yanyushin, G. Bernát, D.V. Zlenko, P.M. Krasilnikov, E.P. Lukashev, E.G. Maksimov, V.Z. Paschenko, Fluorescence quenching of the phycobilisome terminal emitter L_CM from the cyanobacterium *Synechocystis* sp. PCC 6803 detected *in vivo* and *in vitro*, Photochem. Photobiol. B: Biol. 125 (2013) 137–145.
[80] I.N. Stadnichuk, P.M. Krasilnikov, D.V. Zlenko, A.Y. Freidzon, M.F. Yanyushin, A.B. Rubin, Electronic coupling of the phycobilisome with the orange carotenoid protein and fluorescence quenching, Photosynth. Res. 124 (2015) 315–335.
[81] B.V. Trubitsin, V.V. Ptushenko, O.A. Koksharova, M.D. Mamedov, L.A. Vitukhnovskay, I.A. Grigorev, A.Y. Semenov, A.N. Tikhonov, EPR study of electron transport in the cyanobacterium *Synechocystis* sp. PCC 6803: oxygen-dependent interrelations between photosynthetic and respiratory electron transport chains, Biochim. Biophys. Acta 1708 (2005) 238–249.
[82] L.E. Page, M. Liberton, H.B. Pakrasi, Reduction of photoautotrophic productivity in the cyanobacterium *Synechocystis* sp. strain PCC 6803 by phycobilisome antenna truncation, Appl. Environ. Microbiol. 78 (2012) 6349–6351.
[83] M. Mimuro, C. Lipschultz, E. Gantt, Energy flow in the phycobilisome core of *Nostoc* sp. (MAC): two independent terminal pigments, Biochim. Biophys. Acta 852 (1986) 126–132.
[84] D.J. Lundell, A.N. Glazer, Molecular architecture of a light-harvesting antenna. Core substructure in *Synechococcus* 6301 phycobilisomes: quaternary interaction in the *Synechococcus* 6301 phycobilisome core as revealed by partial tryptic digestion and circular dichroism studies, J. Biol. Chem. 258 (1983) 8708–8713.
[85] J. Zhao, J. Zhou, D.A. Bryant, Energy transfer processes in phycobilisomes as deduced from analyses of mutants of *Synechococcus* sp. PCC 7002, in: N. Murata (Ed.), Research in Photosynthesis, vol. 1, Kluwer, Dordrecht, 1992, pp. 25–32.
[86] M.K. Ashby, C.W. Mullineaux, The role of ApcD and ApcF in energy transfer from phycobilisomes to PS I and PS II in a cyanobacterium, Photosynth. Res. 61 (1999) 169–179.
[87] D.V. Zlenko, P.M. Krasilnikov, I.N. Stadnichuk, Structural modeling of the phycobilisome core and its association with the photosystems, Photosynth. Res. 130 (2016) 347–356.